JOURNAL OF SOLID STATE CHEMISTRY 98, 301–311 (1992)

Structural Mechanisms in the Bismuth Strontium Cuprates: HREM Study of Domains and Boundaries in Tubular Phases

M. T. CALDÈS,* M. HERVIEU, A. FUERTES,* AND B. RAVEAU

*Laboratoire de Cristallographie et Sciences des Matériaux, I.S.M.Ra Boulevard du Maréchal Juin, 14050 Caen Cedex, France, and *Institut de Ciencias de Materiales, Campus UAB-08193-Bellaterra-Barcelona-Spain*

Received July 17, 1991; in revised form December 2, 1991

Four families of bismuth layered cuprates exhibit a structure closely related to that of the ideal "2201" superconductor. The HREM study of the "tubular phases" $(Bi_{2-x}Sr_{2-x}CuO_6)_n(Sr_{8-x'}Cu_6O_{16+y})$ showed that numerous domains arise in the crystals, as a result of the setting up of structural mechanisms similar to those involved in the stabilization of the different "2201"-related phases. The structural relationships between the different families are discussed.

The discovery of superconductivity in the "2201" bismuth cuprate (*1*) which corresponds to the theoritical formula $Bi_2Sr_2CuO_6$ has encouraged the explorations of the system Bi–Sr–Cu–O. The results obtained these last 4 years have rapidly shown that the crystal chemistry of these oxides is very complex. The "2201" compound itself is far from being completely understood (*2–9*); two monoclinic forms have been observed (*5–7*), closely related from the structural view point, one being a superconductor, the other being an insulator; nevertheless, the superconducting phase differs from the insulating phase by modulation phenomena. Moreover the exact compositions, especially the molar ratio Bi/Sr, and the oxygen content of these two forms are not known with accuracy. Recently a new family of insulating oxides, $(Bi_{2+x}Sr_{2-x}CuO_6)_n \cdot (Sr_{8-x'}Cu_6O_{16+y})$, called the "tubular phases" has been characterized for $n = 4$ to 7 (*12–14*). The latter oxides exhibit an orthorhombic symmetry and a structure closely related to that of the superconducting "2201"-type oxide. Besides these orthorhombic tubular phases, a monoclinic form has also been obtained for $n = 7$ (*15*). We report here on the structural relationships between these different oxides and the different mechanisms involved in the formation of domains observed by high resolution electron microscopy.

Structural Relationships in the System Bi–Sr–Cu–O

The four types of phases isolated in the Bi–Sr–Cu–O system are all closely related to each other and can be described as derived from an ideal structure of the oxide "$Bi_2Sr_2CuO_6$." Such an ideal "2201" oxide corresponds to the regular intergrowth of triple rock salt layers $[(BiO)_2SrO]_\infty$ with single octahedral perovskite layers $[SrCuO_3]_\infty$ (Fig. 1a); this ideal structure should be tetragonal $I4/mmm$ with $a \approx a_p$

0022-4596/92 $5.00

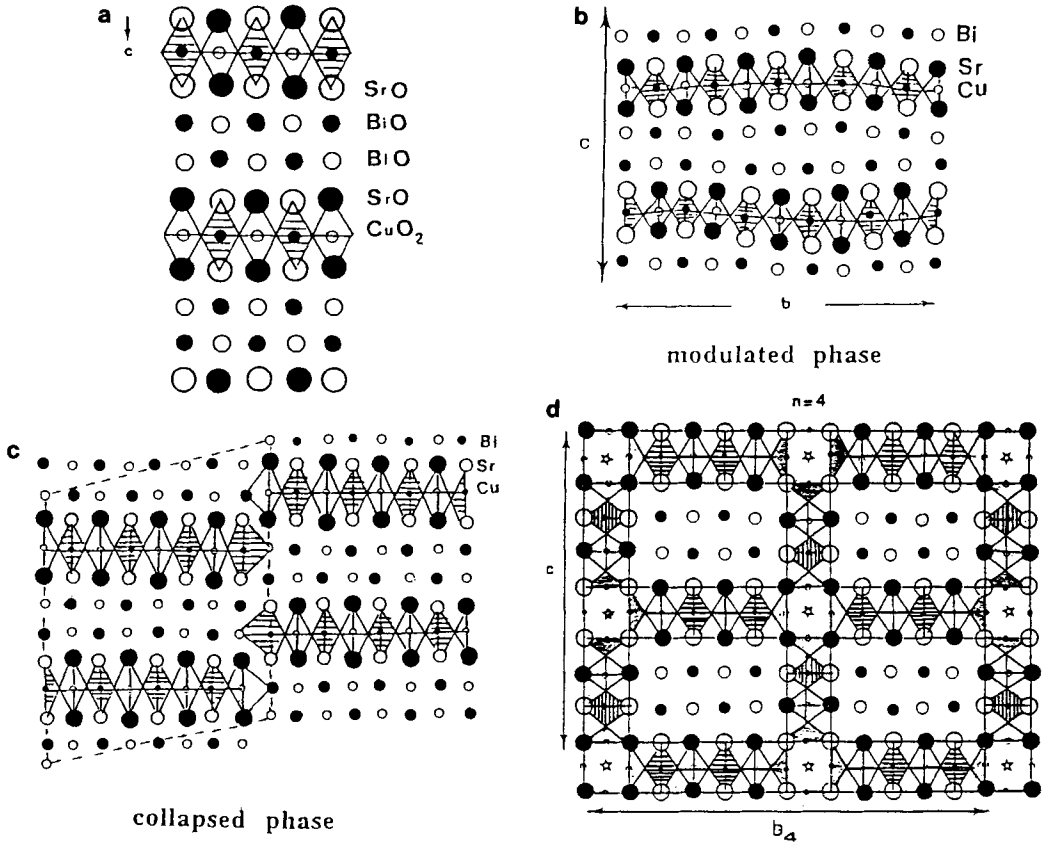

FIG. 1. Schematical projection along $[110]_p$ of: (a) ideal "2201" structure built up from the intergrowth of triple rock-salt layers and single perovskite layer; (b) modulated "2201" phase; (c) collapsed "2201" phase, according to (*6*); (d) $n = 4$ orthorhombic tubular phase; (e) $n = 6$ orthorhombic tubular phase; (f) $n = 5$ orthorhombic tubular phase; (g) $n = 7$ orthorhombic tubular phase; (h) $n = 7$ monoclinic tubular phase.

and $c \approx 24$ Å (a_p: parameter of the cubic cell of the perovskite). In fact this symmetry, which has been observed for the phase $Tl_2Ba_2CuO_6$ (*10, 11*), does not exist for $Bi_2Sr_2CuO_6$.

The Monoclinic or "Pseudo-orthorhombic" "2201" Superconductor

This phase, which was found to be a superconductor at 22 K (*1*), exhibits an orthorhombic average subcell characterized by the relations $a \approx b \approx a_p\sqrt{2}$ and $c \approx 24$ Å; it also exists as an insulating phase which is supposed to differ from the superconductive phase by the Bi/Sr ratio. In fact, the symmetry of the actual structure is monoclinic and the E.D. patterns (*1, 2, 16–18*) show the existence of incommensurate satellites. The bidimensionnal modulation is characterized by a variation of the direction of the vector of modulation and variation of the wavelength with composition (*6*), the q value ranging from 4.7 to 5. Thus this structure can be described as derived from the ideal "2201" structure by a modulated displacement of the cations correlated with a

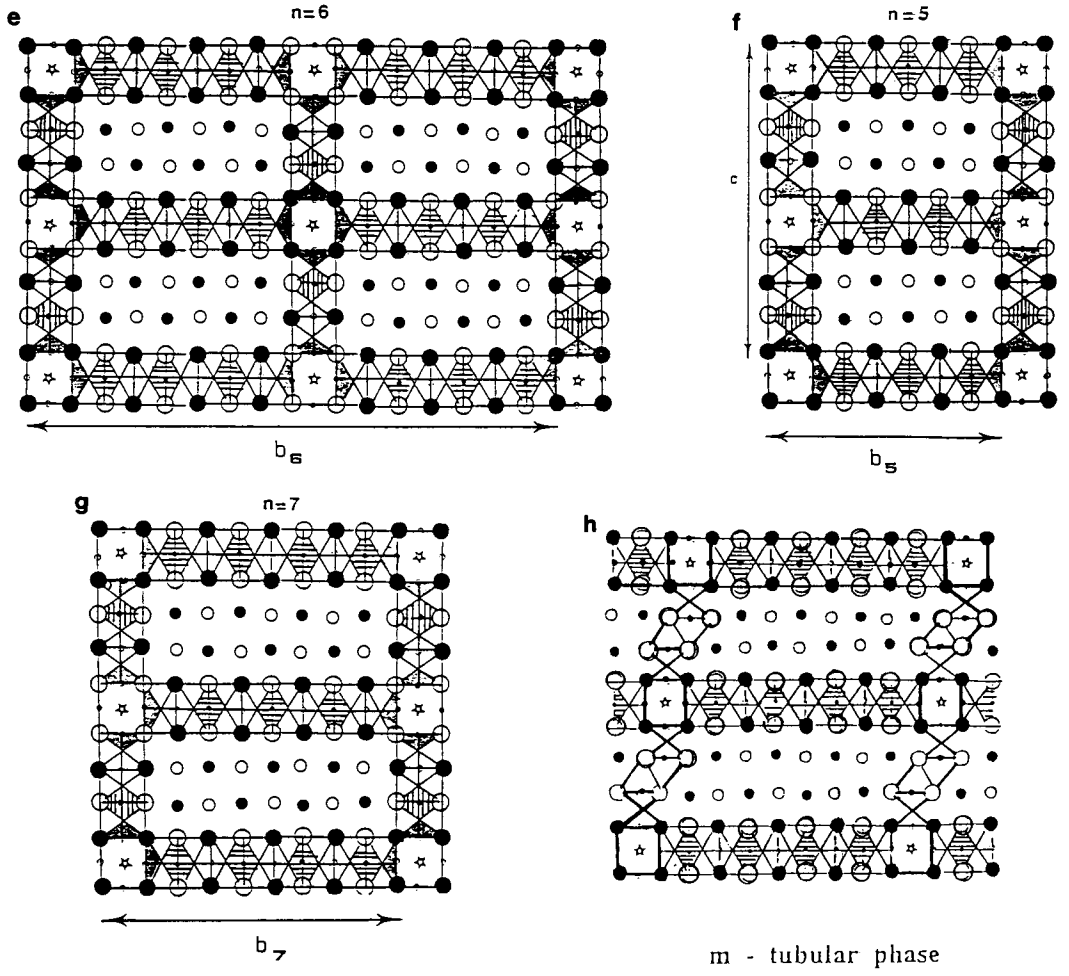

FIG. 1—*Continued*

modulated distribution of these cations (Fig. 1b).

Up to now the incommensurate structure of this phase has not been resolved, owing to the difficulty to prepare crystals of good quality. However, preliminary analyses made by different authors (*2–11*) suggest that this oxide exhibits a bismuth and a copper excess and a strontium deficiency with respect to the ideal formula $Bi_2Sr_2CuO_6$. Single crystal studies of this phase, actually in progress (*19*), show without ambiguity that the Bi/Sr ratio differs significantly from 1($\approx$1.13). Moreover, it is not possible to know the exact oxygen stoichiometry of this phase from the structural study, up to now, owing to the modulated character of the structure and especially to the "disordering" observed in the "BiO" layers. Thus this oxide can be formulated $Bi_{2+x}Sr_{2-x}CuO_{6\pm\delta}$.

The Monoclinic "Collapsed" "2201" Insulating Phase

Remaining near the "2201" stoichiometry but increasing significantly the stron-

tium content with respect to copper so that Bi + Sr is in excess with respect to the formula $Bi_2Sr_2CuO_6$, one obtains a monoclinic phase (*5–8*), also related to that of the ideal $Bi_2Sr_2CuO_6$, with the following parameters: $a = 24.47$ Å, $b = 5.42$ Å, $c = 21.96$ Å, $\beta = 105°4$. This form, called the "collapsed phase," results from a shearing mechanism along **b** in the monoclinic modulated "2201" phase (*6*). It corresponds indeed to a translation along **c** of 4.6 Å of one "2201" ideal block (eight octahedra wide) with respect to the adjacent one (Fig. 1c). It results that the copper layers are interrupted in the (001) plane whereas the rock-salt layers zig-zag.

As far the structure of this phase is not determined from a single crystal study, it is not possible to give its exact formula for cations as well as for oxygen.

The Orthorhombic "Tubular" Phases $(Bi_{2+x}Sr_{2-x}CuO_6)_n(Sr_{8-x'}Cu_6O_{16+y})$

These phases have been synthesized for an excess of strontium and copper with respect to the formula $Bi_2Sr_2CuO_6$ (*12, 13*). The structures of these different members, (Figs. 1d–g) can be deduced from the "2201" ideal oxide by an intergrowth mechanism along **b**, according to the formula $(Bi_{2+x}Sr_{2-x}CuO_6)_n \cdot (Sr_{8-x'}Cu_6O_{16+y})$; in fact, the two intergrown structural units consist of one ideal "2201"-type slab, which is n octahedra wide, with one perovskite-related slice $[Sr_{8-x}Cu_6O_{16+y}]_\infty$ involving "Cu_4Sr_4"" square shape units.

The parameters of the orthorhombic cell of these oxides are related to a_p in the following way (*12*):

n: even $\quad a = 2a_p\sqrt{2}$

n: uneven $\quad a = 2a_p\sqrt{2}$

$$b = \left[(n+1)a_p\frac{\sqrt{2}}{2} + a_p\right] \times 2$$

$$b = (n+1)a_p\frac{\sqrt{2}}{2} + a_p$$

$$c = [a_p + 3/2a_p\sqrt{2}] \times 2 \approx 24 \text{ Å}$$

$$c = [a_p + 3/2a_p\sqrt{2}] \times 2 \approx 24 \text{ Å}.$$

The Monoclinic Tubular Phase $(Bi_{2+x}Sr_{2-x}CuO_6)_7 \cdot (Sr_{8-x'}Cu_6O_{16+y})$

Starting from the orthorhombic tubular phase $(Bi_{2+x}Sr_{2-x}CuO_6)_7 \cdot (Sr_{8-x'}Cu_6O_{16+y})$, a shifting mechanism along **b** of one perovskite related slab, $[Sr_{8-x'}Cu_6O_{16+y}]_\infty$, out of two leads to a monoclinic tubular phase (Fig. 1h) with the following parameters (13):

$$a \approx 5.4 \text{ Å} \quad b \approx 24.7 \text{ Å}$$

$$c \approx 24.65 \text{ Å} \quad \alpha \approx 96°.$$

The structure of such a phase can be described as a regular intergrowth of three tubular members with $n = 6$, 7, and 8 (*15*).

Though it is the only monoclinic tubular phase observed up to now, the possibility of synthesis of the other members of the series should be considered.

Domains and Boundaries in the $n = 7$ Tubular Phases

The close relationships between these different structures suggest the possibility of numerous extended defects. This is the case of tubular phases for which HREM observations show the formation of complex domains.

FIG. 2. (a) [001] electron diffraction pattern and (b) high resolution image of 90° oriented domains. (c) These domains are adjacent in the *ab* plane contrary to the modulated 2201 (d) where the lamellae are superposed; (e) ideal drawing of the domains projected along [001]. In the 2201 slices, Bi, Sr, and Cu are projected over the same position (stars). In the perovskite related slice, labeled P, strontium and copper atoms are projected over the same position (black dots). The small black dots are copper atoms.

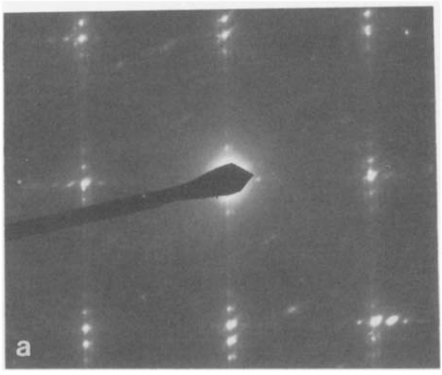

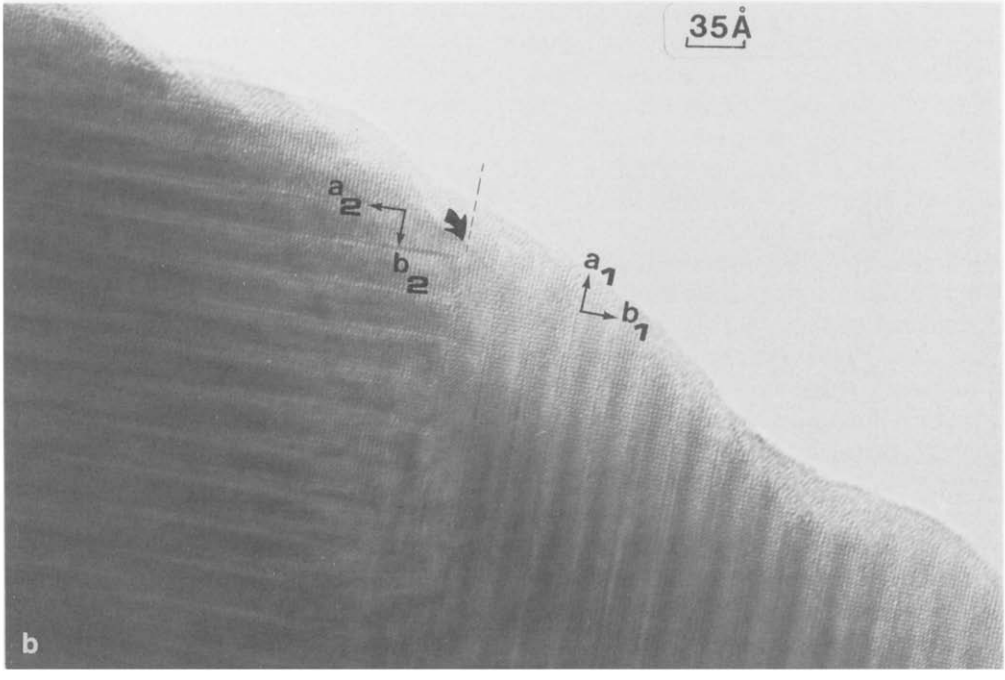

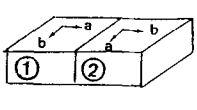

c

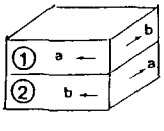

d

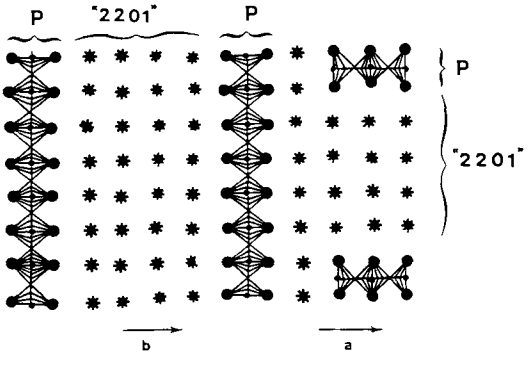

e

As previously reported (*15*), arcing of the spots in the E.D. patterns of the $n = 7$ tubular member and superposition of orthorhombic and monoclinic patterns are frequent phenomena. They result from the existence of slightly misoriented domains which are described here.

90°-Oriented Domains

The first type of domains corresponds to an intergrowth mechanism taking place along two equivalent directions of the subcell of the "2201" ideal structure. This is observed on E.D. patterns (Fig. 2a) and the corresponding image (Fig. 2b) of the $n = 7$ member of the orthorhombic tubular phases. On the edge of the crystal the boundary between the two domains, labeled 1 and 2, is parallel to $(100)_2$ and $(010)_1$, respectively, but it can be seen that in the bulk (Fig. 2b) the boundary is not a simple plane and becomes more complex. The existence of 90°-oriented domains was also reported in the "2201" superconductor (*20–22*). However, the disposition of the adjacent domains is different in the two oxides, owing to the different nature of the structural features which generate the superstructure along the **b** axis. In the "2201" oxide, the 90°-oriented domains correspond generally to the superposition of lamellae along **c** (Fig. 2d), contrary to the tubular phases where the lamellae are formed from adjacent domains (Fig. 2c). A model of the atomic arrangement of two adjacent domains is shown in Fig. 2e; both domains are viewed along [001] so that all the atoms of "2201" slab (Bi–Sr–Cu and O) are projected over the same position (stars), whereas in the perovskite slab only Sr and O atoms are superposed. It appears clearly from this schema that two $[Sr_{8-x}Cu_6O_{16+y}]_\infty$ layers can have their origin in the same "2201" unit and be oriented at 90°, without any strong distortion of the structure of the domains. As a result, the ideal "2201" layers which are seven octahedra wide are oriented at 90° in the two domains, one "2201" layer playing the role of the boundary. The generation of such adjacent domains is a common feature in perovskite-related compounds, where a supercell is observed from an ion ordering or an intergrowth mechanism; the fact that they are not observed in the modulated "2201" phase could be correlated to the strong undulations of the atomic planes which prevent an easy junction between the domains to be ensured.

A second type of 90°-oriented domains is observed in the tubular phases, which is generated by a mechanism closely related to the previous one. An example for $n = 4$ is shown in Fig. 3a. The interface between the two domains corresponds, in the same way, to the perovskite-related layers but, in that type of 90°-oriented domains, $\mathbf{b}_1$ remains parallel to $\mathbf{b}_2$, whereas $\mathbf{c}_1$ and $\mathbf{a}_2$ become parallel (Fig. 3b). The idealized model of such a junction is shown in Fig. 3c; the right domain being viewed along [001], the stars symbolize the different cations of the "2201" slice projected over the same position.

Ill-Crystallized Boundaries

The mica-like character of the tubular phase as soon as n is greater than 4 (*12*) leads to the formation of lamellae some 100 Å wide. The interfaces between two adjacent lamellae consist in strips of more or less crystallized material. An example is shown in Fig. 4, where the regular arrangement of the structural units of the tubular phase is destroyed; it appears clearly that atomic layers, whose number increases from the edge of the crystal to the bulk, are still observed in that case. It should be noted that an undulating behavior of the additional layers, similar to that observed in the modulated phases, can be observed when the conditions of imaging are good enough in the disturbed area (Fig. 4).

Similar phenomena have been reported in

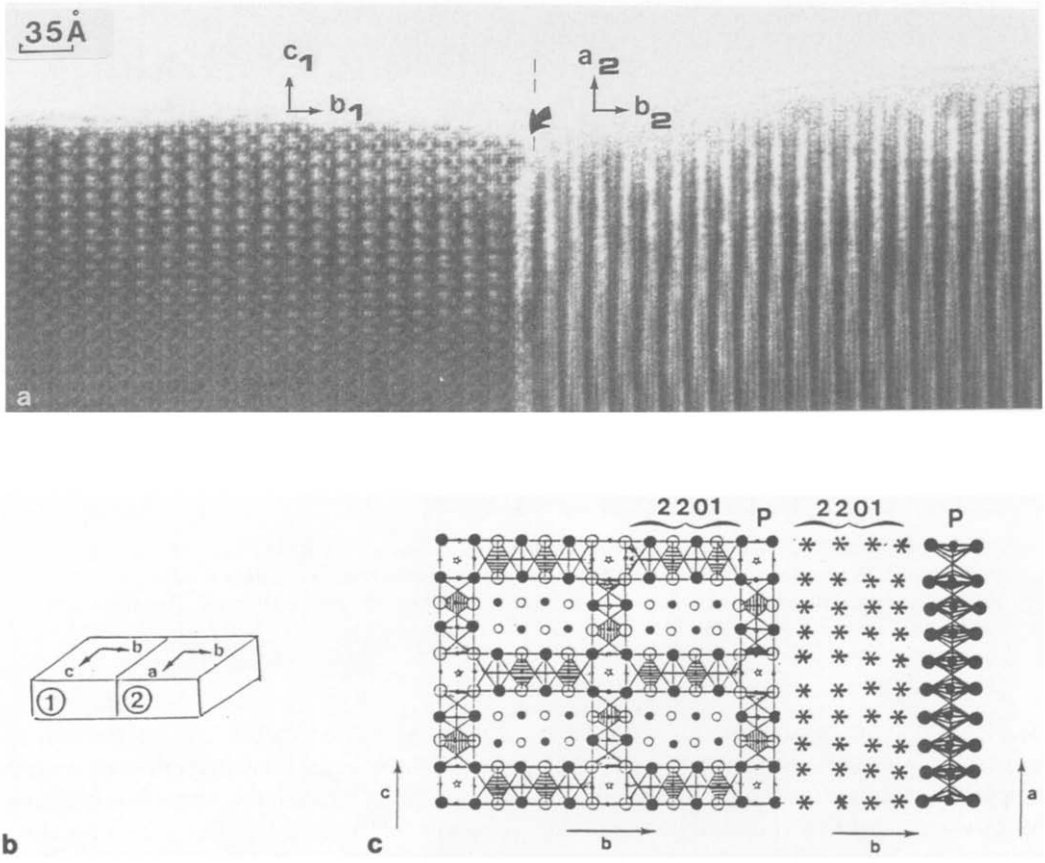

FIG. 3. Second type of 90° oriented domains: (a) HREM image, (b) relative position of the domains, and (c) idealized model of the junction. Symbols for atoms are identical to Fig. 2e in the [001] projection of the structure.

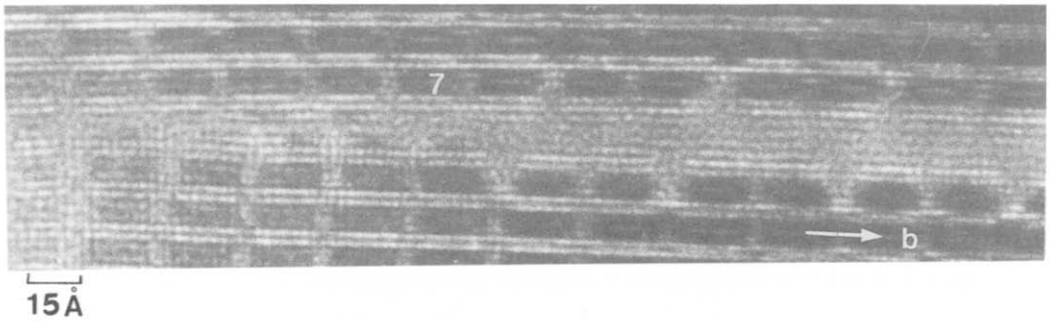

FIG. 4. A mica-like morphology is observed in the tubular phases. The interfaces between the lamellae consist in strips of more or less crystallized material.

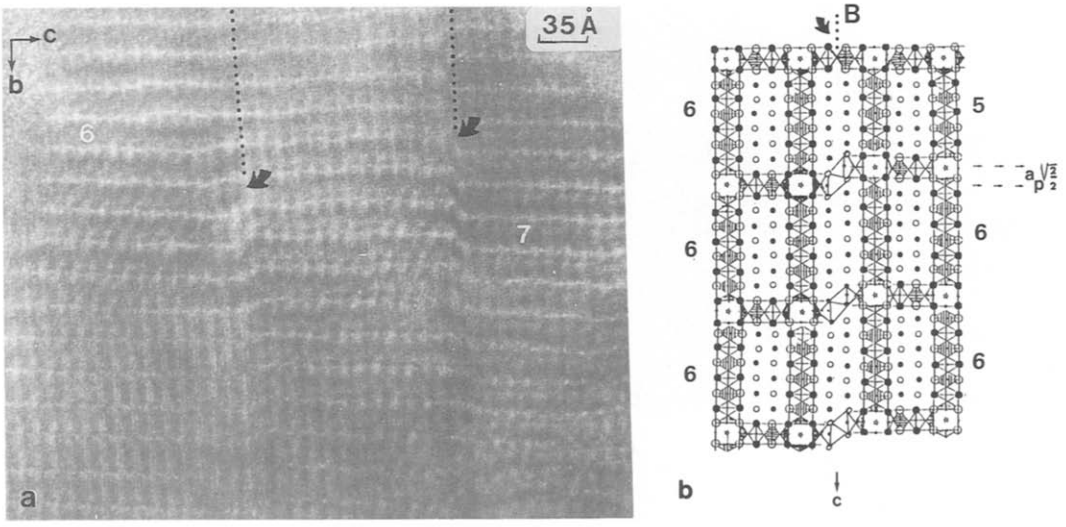

FIG. 5. Example of domains resulting from a shearing mechanism. (a) HREM image. The boundaries (arrowed dotted lines) are parallel to (001) and arise from the existence of different n values. (b) They involve a mechanism similar to that observed in the monoclinic tubular phases (Fig. 1h). The translation amplitude is $\Delta n \times a_p \times (\sqrt{2}/2)$; here $\Delta n = 1$.

the bismuth superconductors (*23*); they are the result of the mica-like morphology of the samples and they are one of the origins of the misorientation of the lamellae and the arcing of the spots observed in the electron diffraction patterns.

Shearing Domains

Two types of domains resulting from shearing mechanisms were observed:

The first one is illustrated in Fig. 5a; boundaries parallel to (001) cross the crystals and generate domains of 100 or 200 Å wide. In this image the white lines parallel to **c** are associated with the $[Sr_8Cu_6O_{16}]_\infty$ slices; it can be seen that they are shifted along **b** through the boundaries (dotted lines). At the level of the boundary, the $[Sr_4Cu_4]$ squared units of two adjacent slices appear to be translated. Such a translation corresponds to the mechanism which caused the orthorhombic–monoclinic transition in tubular phases (Figs. 1g, 1h). However, the amplitude of the translation, which is equal to $a_p(\sqrt{2}/2)$ in the monoclinic phase, is greater through such boundaries and is, moreover, variable along one boundary. The origin of this variation along the boundary is due to the presence of members of different n values on both sides of the boundary; in that way, the translation can be equal up to $4 \times a_p\sqrt{2}/2$. A structural model for such a boundary is proposed in Fig. 5b. The idealized drawing shows how a defective number ($n' = 5$ in an $n = 6$ matrix in that example) involves a shifting of the double bismuth layers; on both sides of these shifted layers, which play the role of boundary (noted B), the $[Sr–Cu–Sr]_4$ squares are shifted. It can be seen that, in a general way, a variation $\Delta n = n\text{-}n'$ of the thickness of the "2201" slice implies a translation $\Delta n \times a_p(\sqrt{2}/2)$.

In the second type of domain, shown in Fig. 6a, the bismuth layers are interrupted at the level of the boundary and shifted along the **c** axis; the boundary is parallel

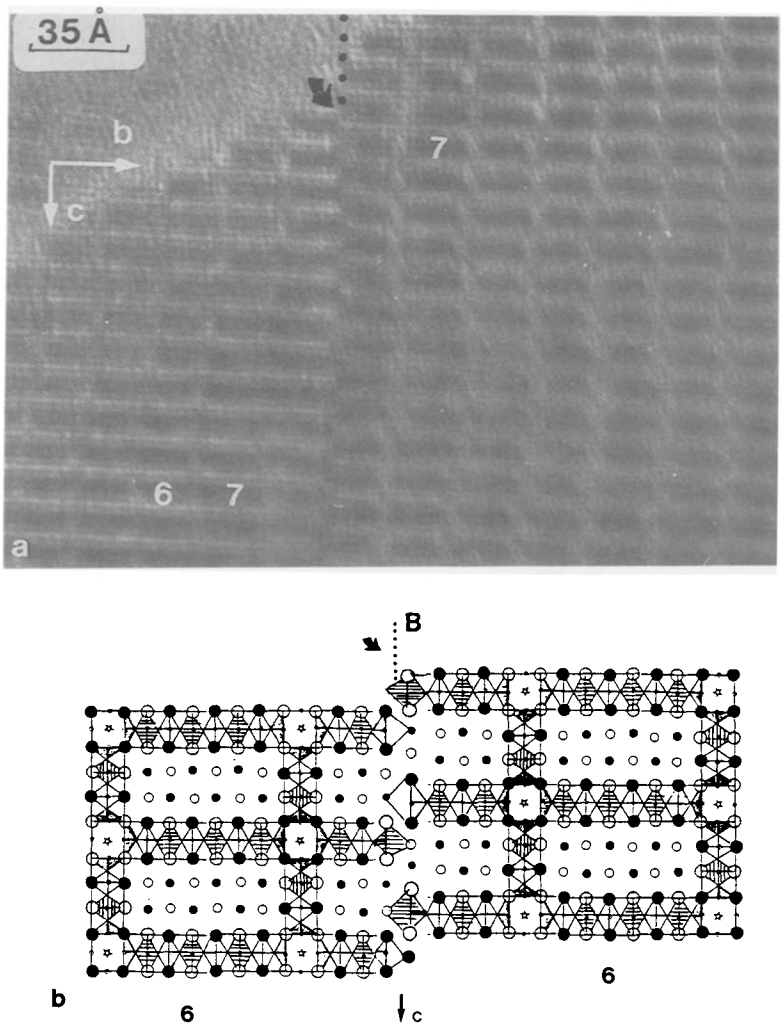

FIG. 6. Example of domains resulting from a shearing mechanism similar to that observed in the collapsed phase (Fig. 1c). (a) HREM image. The boundary (arrowed dotted line) is parallel to (010). (b) Idealized model of the junction.

to (010). It can be seen that, at the level of the boundary, the $[Sr_8Cu_6O_{16}]_\infty$ slices (white lines parallel to **c**) disappear so that the shifting occurs in the core of the "2201" slices. The amplitude of the translation is close to 4.6 Å. The direction and the amplitude of this translation show that the mechanism involved in that boundary is similar to that which governs the monoclinic collapsed "2201" phase (Fig. 1c); an idealized model is given in Fig. 6b. Taking into account the hypothetical structure proposed for this phase (*6*), a shifting is observed along **c** which involves the connection of $[BiO]_\infty$ layers with $[SrO]_\infty$ or $[CuO_2]_\infty$ layers through the boundary (noted B).

Discussion and Concluding Remarks

An interesting point to note deals with the upper limit value of the "b" parameters. In

the monoclinic collapsed phase one observes a periodicity of $4 \times a_p\sqrt{2}$ along that direction, whereas in the orthorhombic tubular structures the highest periodicity in single phase does not overpass that of the $n = 7$ member, i.e., close to 25 Å. In the monoclinic modulated "2201" oxide, the modulation modes (magnitude and angle of modulation vector in the (100) plane) vary significantly with Bi/Sr ratio and oxygen content, but the q value ranging from 4.65 to 5 corresponds to periodicities ranging from 25.2 to 27 Å. Thus, in these four phases with a structural mechanism set up along the **b** axis (modulation, intergrowth, or shearing), the highest periodicities along **b** range from $4 \times a_p\sqrt{2}$ to $5 \times a_p\sqrt{2}$.

From the HREM study of the "tubular" phases, it appears that nonstoichiometry is accomodated through two main structural features. The first one corresponds to intergrowth defects, arising from the existence of aleatory sequences of n members along **b** and/or **c** axes (*14, 15*). They are classical defects of the structures built up from the intergrowth of two structural units. The second typical phenomenon deals with the fragmentation of the crystals in numerous domains whose boundaries are parallel to (100), (010), or (001) planes. The examination of these domains showed that simple mechanisms such as twinning or antiphase boundaries which are observed in the others superconducting cuprates are not involved in their formation. In fact, the numerous domains which have been observed can be considered as mainly generated by the mechanisms which govern the formation of the four different phases related to the "2201" phase. The boundaries do not consist of one plane which plays the role of mirror, but in relative arrangements of two (or more) adjacent layers, which are not those expected in the structure and which are characteristic of one of the other building mechanisms. It is likely that these defects result from local variations of compositions; owing to the close nominal compositions of the four "2201" parent phases, their structural mechanisms are easily engaged, allowing nonstoichiometry effects to be accomodated.

In conclusion, the results presented in this paper enhance the close relationships between the different bismuth strontium cuprates. The investigation of the nonstoichiometry mechanisms setting up in these matrices can be very beneficial for understanding the structural parameters which govern the superconducting properties of the bismuth cuprates.

Acknowledgments

M.T. Caldes and A. Fuertes acknowledge the Spanish CICYT (Grants Mat. 88-0/63-603 and Mat. 90-1020-602-01) and the MIDAS program for support of this research.

References

1. C. Michel, M. Hervieu, M. M. Borel, A. Grandin, F. Deslandes, J. Provost, and B. Raveau, Z. Phys. B, 68, 421 (1987).
2. J. B. Torrance, Y. Tokura, S. J. La Placa, T. C. Huang, R. J. Savoy, and A. I. Nazzal, *Solid State Commun.* **66,** 703 (1988).
3. R. S. Roth, *in* "Proceedings, American Physical Society Meeting, New Orleans, March, 1988."
4. A. K. Cheetham, A. M. Chippindale, and J. J. Hibble, *Nature* **333,** 21 (1988).
5. R. S. Roth, C. J. Rawn, and I. A. Bendersky, *J. Mater. Res.* **5,** 46 (1990).
6. Z. Hiroi, Y. Ikeda, M. Takano, and Y. Bando, *J. Mater. Res.* **6,** 435 (1991).
7. B. C. Chakoumakos, P. S. Ebey, B. C. Sales, and E. Sonders, *J. Mater. Res.* **4,** 767 (1991).
8. J. A. Saggio, K. Siyata, J. Hahn, S. J. Mwu, K. Poppelmeier, and T. O. Mason, *J. Am. Ceram. Soc.* **72,** 849 (1989).
9. J. Akimitsu, A. Yamazaki, H. Sawa, and M. Fujiki, *Jpn. J. Appl. Phys.* **26,** L208 (1987).
10. C. C. Torardi, M. A. Subramanian, J. C. Calabrese, J. Gopalakrishnan, E. M. Mc Carron, K. J. Morrissey, T. R. Askew, R. B. Flippen, U. Chowdry, and A. W. Sleight, *Phys. Rev. B* **38,** 225 (1988).
11. M. Onoda and M. Saro, *Solid State Commun.* **67,** 799 (1988).
12. A. Fuertes, C. Miratvilles, J. Gonzalez-

CALBET, M. VALLET-REGI, X. OBRADORS, AND J. RODRIGUEZ CARJAVAL, *Physica* **157,** 529 (1989).
13. M. T. CALDES, J. M. NAVARRO, F. PEREZ, M. CARRERA, J. FONTUBERTA, M. CASAÑ PASTOR, C. MIRATVILLES, X. OBRADORS, J. RODRIGUEZ CARJAVAL, J. M. GONZALEZ-CALBET, M. VALLET-REGI, A. GARCIA, AND A. FUERTES, *Chem. Mater.* **3,** 844 (1991).
14. M. T. CALDES, M. HERVIEU, A. FUERTES, B. RAVEAU, *J. Solid State Chem.,* **97,** 48 (1992).
15. M. T. CALDES, M. HERVIEU, A. FUERTES, AND B. RAVEAU, *J. Solid State Chem.,* in press.
16. S. K. BLOWER AND C. GREAVES, *Acta Cryst C* **44,** 587 (1988).
17. G. VAN TENDELOO, H. W. ZANDBERGEN, AND S. AMELINCKX, *Solid State Commun.* **66,** 927 (1988).
18. Y. IKEDA, H. ITO, S. SHIMOMURA, Y. OUE, K. INABA, Z. HIROI, AND M. TAKANO, *Physica C* **159,** 93 (1989).
19. H. LELIGNY, S. DURCOK, P. LABBE, M. LE DESERT AND B. RAVEAU, *Acta Cryst B,* in press.
20. M. HERVIEU, C. MICHEL, B. DOMENGES, Y. LALIGANT, A. LEBAIL, G. FEREY, AND B. RAVEAU, *Mod. Phys. Lett.* **2,** 491 (1988).
21. M. HERVIEU, C. MICHEL, C. MARTIN, AND B. RAVEAU, *Mater. Sci. Eng. B* (1989).
22. Y. MATSUI, H. MAEDA, Y. TANAKA, E. TAKAYAMA-MUROMACHI, S. TAKEKAWA AND S. MORUICHI, *Jpn. J. Appl. Phys.* **27,** L827 (1988).
23. M. HERVIEU, B. DOMENGES, C. MICHEL, AND B. RAVEAU, *Mod. Phys. Lett.* **2,** 6, 835 (1988).